

Controlled Modification of Microstructured Silicon Surfaces for Confinement of Biological Macromolecules and Liquid Crystals

T. Pfohl,[†] J. H. Kim,^{†,‡} M. Yasa,[†] H. P. Miller,[‡] G. C. L. Wong,^{†,#} F. Bringezu,[§] Z. Wen,^{||} L. Wilson,[‡] M. W. Kim,^{†,‡} Y. Li,[†] and C. R. Safinya^{*,†}

Materials Research Laboratory, Materials Department, Physics Department, and Biomolecular Science and Engineering Program, University of California, Santa Barbara, California 93106, Molecular, Cellular, and Developmental Biology Department, University of California, Santa Barbara, California 93106, Department of Chemical Engineering, University of California, Santa Barbara, California 93106, Department of Optoelectronic Instruments, Chongqing University, Chongqing, China, and Department of Physics, Korea Advanced Institute of Science and Technology, Taejon 305-701, Korea

Received January 29, 2001. In Final Form: May 30, 2001

We report new methods of surface modifications for confining and aligning biological macromolecules and liquid crystals on microstructured surfaces. Microcontact printing and polyelectrolyte adsorption were used to pattern and control surface properties of silicon microchannels fabricated by photolithography and etching. We show that the wettability inside and on top of the microstructures can be independently varied by selective deposition of a hydrophobic monolayer using microcontact printing, whereas the surface charge, reactivity, and biocompatibility in the microchannels can be adjusted by adsorbing polyelectrolytes to the surface. A near ideal contrast in surface properties was achieved by microcontact printing on preadsorbed polyelectrolyte layers. Three-dimensional laser scanning confocal microscopy was used to characterize the wetting behavior of biological macromolecules (lipids, DNA, microtubules) confined in the microstructures. DNA molecules in concentrated solutions were observed to orient along the microchannels, as a result of surface confinement, when their contour length approached the width of the microchannels. We demonstrate that the surface microstructures may be used to control the mesoscopic defect structures and defect sizes of liquid crystals by studying the defect structure of 8CB (4'-n-octyl-4-cyanobiphenyl) as a function of the widths and depths of the microchannels. The order induced due to microchannel confinement of biological molecules has the potential of resulting in unique structure characterization of highly oriented biological macromolecules using synchrotron X-ray microdiffraction methods.

Introduction

Surfaces that exhibit defined patterns of contrasting properties, such as wettability, chemical reactivity, and surface charge, on the micrometer and submicrometer scale, have recently received tremendous attention. Micropatterning plays an important role in biology and bioengineering research for miniaturization and control of bioreactors and biosensors,^{1–3} adsorption of proteins and cells on selected surfaces,^{4–7} and investigation of cell

growth on structured semiconductors.^{8,9} In these experiments, biological molecules or cells adsorb on specific structured surfaces from a solution above the surface or solutions are directed through microchannel systems that are in contact with a macroscopic reservoir of liquid. Thus, one focus of experimental^{10–12} and theoretical^{13,14} studies has been on elucidating the wetting properties on structured surfaces in order to better understand the properties of the biomolecules and cells on patterned surfaces.

In this paper, we present studies aimed at controlling the volume and composition of a solution at the picoliter scale in silicon microstructures. Patterned surfaces with micrometer-size features were created using a combination of photolithography and etching,¹⁵ microcontact print-

* Corresponding author.

[†] Materials Research Laboratory, Materials Department, Physics Department, and Biomolecular Science and Engineering Program, University of California.

[‡] Molecular, Cellular, and Developmental Biology Department, University of California.

[§] Department of Chemical Engineering, University of California.

^{||} Department of Optoelectronic Instruments, Chongqing University.

[†] Department of Physics, Korea Advanced Institute of Science and Technology.

[#] Present address: Department of Materials Science and Engineering and Physics Department, University of Illinois, Urbana-Champaign, IL 61801.

(1) Service, R. F. *Science* **1998**, *282*, 396.

(2) Burns, M. A.; Johnson, B. N.; Brahmasandra, S. N.; Handique, K.; Webster, J. R.; Krishnan, M.; Sammarco, T. S.; Man, P. M.; Jones, D.; Heldsinger, D.; Mastrangelo, C. H.; Burke D. T. *Science* **1998**, *282*, 484.

(3) Han, J.; Craighead, H. G. *Science* **2000**, *288*, 1026.

(4) Zhang, S. G.; Yan, L.; Altman, M.; Lassle, M.; Nugent, H.; Frankel, F.; Lauffenburger, D. A.; Whitesides, G. M.; Rich, A. *Biomaterials* **1999**, *20*, 1213.

(5) Braun, D.; Fromherz, P. *Phys. Rev. Lett.* **1998**, *81*, 5241.

(6) Delamarche, E.; Bernard, A.; Schmid, H.; Michel, B.; Biebuyck, H. *Science* **1997**, *276*, 779.

(7) Bernard, A.; Renault, J. P.; Michel, B.; Bosshard, H. R.; Delamarche, E. *Adv. Mater.* **2000**, *12*, 1067.

(8) Craighead, H. G.; Turner, S. W.; Davis, R. C.; James, C.; Perez, A. M.; St. John, P. M.; Isaacson, M. S.; Kam, L.; Shain, W.; Turner, J. N.; Banker, G. J. *Biomed. Microdev.* **1998**, *1*, 49.

(9) Dike, L. E.; Chen, C. S.; Mrkisch, M.; Tien, J.; Whitesides, G. M.; Ingber, D. E. *In vitro Cell Dev. Biol.: Anim.* **1999**, *35*, 441.

(10) Gau, H.; Herminghaus, S.; Lenz, P.; Lipowsky, R. *Science* **1999**, *283*, 46.

(11) Herminghaus, S.; Fery, A.; Schlagowski, S.; Jacobs, K.; Seemann, R.; Gau, H.; Mönch, W.; Pompe, T. *J. Phys.: Condens. Matter* **1999**, *11*, 57.

(12) van Oudenaarden, A.; Boxer, S. G. *Science* **1999**, *285*, 1046.

(13) Lipowsky, R.; Lenz, P.; Swain, P. S. *Colloids Surf., A* **2000**, *161*, 3.

(14) Bauer, C.; Dietrich, S. *Phys. Rev. E* **1999**, *60*, 6919.

(15) Caine, E. J.; Shi, S.; Hu, E. L.; Idziak, S. H.; Subramanian, G.; Safinya, C. R. *Microelectron. Eng.* **1997**, *35*, 289.

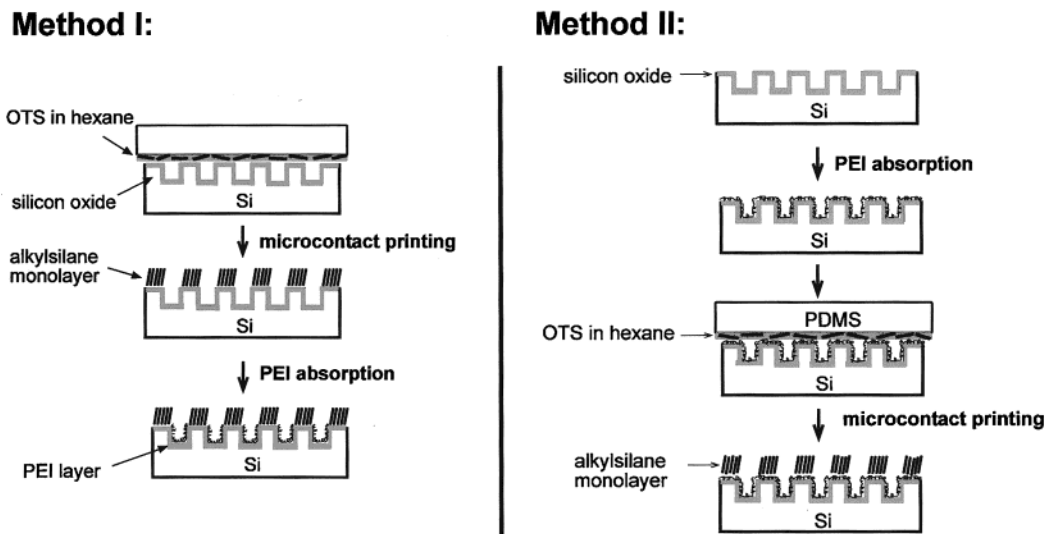


Figure 1. An illustration of the steps used in the surface modification of the lithographic silicon substrates. Method I: First, the hydrophobic monolayer is stamped on the top of the microchannels using microcontact printing. Second, the wall and bottom of the microchannel is coated with PEI. Method II: First, the entire lithographic silicon surface is coated with PEI. Second, the hydrophobic monolayer is stamped on top of the PEI-coated microchannels.

ing,^{16,17} and polyelectrolyte adsorption.¹⁸ These techniques allow us to alter the surface charge, surface reactivity, wettability, and biocompatibility of the microstructures. A micromanipulation/microinjection system was used to fill and control the composition of a solution in a single lithographic microchannel. Using this new technique, we found that biological molecules could be aligned in micron-size channels if the width and/or depth of the microchannel was on the order of a typical macromolecular length. For the case of dilute solutions of biopolymers, the relevant length scale is the persistence length. For the case of concentrated solutions of the biopolymer DNA, we have found that the relevant length scale is the contour length.

Several applications of the microchannel-based confinement and alignment of macromolecules are envisioned. First, highly oriented biopolymer samples can be used as templates for making inorganic materials with desired microporosity. Second, by expanding the investigation to simple liquids and liquid crystalline systems, general wetting behavior on microstructures and the influence of the confinement on material properties could be studied. The methods and techniques presented here are directly applicable in the development of microfabricated devices that detect and analyze macromolecules and biological materials. Third, and in some sense most significantly, the confinement of these biological macromolecules leads to highly ordered systems which will allow structure studies of oriented supramolecular assemblies using X-ray microdiffraction methods without the loss of structural information due to powder averaging introduced because of unoriented samples.^{19,20} Specific examples include recently discovered liquid crystalline structures of the synthetic gene carrier cationic lipid-DNA (CL-DNA) complexes^{21–23} as well as lipid complexes containing polypeptides and filamentous actin.^{24,25} We expect that the preparation of these lipid-polyelectrolyte systems, and

more generally of biological macromolecules, on patterned surfaces will lead to highly oriented samples for structure studies by X-ray microdiffraction methods.

Materials and Methods

Substrate Preparation. The microchannels were fabricated on (100) Si substrates using photolithography and chemical (HF) etching methods. Channel widths range from 1.5–20 μm with 1 mm \times 1 mm area and 1–7 μm depth. Before further surface treatment, the silicon substrates were cleaned in an aqueous $\text{NH}_3/\text{H}_2\text{O}_2$ solution at 80 $^\circ\text{C}$ for 15 min²⁶ and stored afterward in Millipore water (resistance > 18.2 M Ω).

Surface Modifications. The wetting contrast, surface charge, and surface activity of the lithographically fabricated silicon microchannels were controlled by preparing the channel surfaces using two different pathways, which are illustrated in Figure 1.

Method I. Flat poly(dimethylsiloxane) (PDMS) stamps were cast from a planar silicon surface. A solution of 1–2 mM of octadecyltrichlorosilane (OTS, Aldrich) in dry hexane (Aldrich) was used as the “ink” for microcontact printing. A “stamp pad” (planar PDMS stamp) was inked for 10 s with the OTS solution. After the stamp pad was dried for 30 s in a stream of nitrogen, a second stamp was placed atop the surface of the pad with light pressure and the two pads were left in contact for 10 s. This second stamp was used for printing on the silicon surfaces with a \sim 2–3 nm native oxide layer. After 20–30 min, the stamp was removed and the substrate was sonicated for 3–5 min in ethanol and then for 3–5 min in Millipore water. This “dry” stamp pad technique¹⁷ was chosen to avoid capillary condensation and a chemical reaction between excess OTS and the channel inside surfaces (walls and the bottom) during the cleaning process. For the formation of a polyelectrolyte monolayer in the microchannels, the substrate was immersed in a 1 mg/mL aqueous solution of positively charged poly(ethylene imine) (PEI, pH 10, $M_w = 750\,000$, Aldrich) for 20 min and sonicated afterward three times in Millipore water for 2 min.²⁷

(21) Raedler, J. O.; Koltover, I.; Salditt, T.; Safinya, C. R. *Science* **1997**, *275*, 810.

(22) Salditt, T.; Koltover, I.; Raedler, J. O.; Safinya, C. R. *Phys. Rev. Lett.* **1997**, *79*, 2582.

(23) Koltover, I.; Salditt, T.; Safinya, C. R. *Science* **1998**, *281*, 78.

(24) Subramanian, G.; Hjelm, R. P.; Deming, T. J.; Smith, G. S.; Li, Y.; Safinya, C. R. *J. Am. Chem. Soc.* **2000**, *122*, 26.

(25) Wong, G. C. L.; Tang, J. X.; Lin, A.; Li, Y.; Janmey, P. A.; Safinya, C. R. *Science* **2000**, *288*, 2035.

(26) Graf, K.; Riegler, H. *Colloids Surf., A* **1998**, *131*, 215.

(27) Clark, S. L.; Montague, M. F.; Hammond, P. T. *Macromolecules* **1997**, *30*, 7237.

(16) Xia, Y.; Whitesides, G. M. *Angew. Chem., Int. Ed. Engl.* **1998**, *37*, 551.

(17) Pompe, T.; Fery, A.; Herminghaus, S.; Kriele, A.; Lorenz, H.; Kotthaus, J. P. *Langmuir* **1999**, *15*, 2398.

(18) Decher, G. *Science* **1997**, *277*, 289.

(19) Wong, G. C. L.; Li, Y.; Koltover, I.; Safinya, C. R.; Cai, Z. H.; Yun, W. B. *Appl. Phys. Lett.* **1998**, *73*, 2042.

(20) Li, Y.; Wong, G. C. L.; Case, R.; Caine, E.; Hu, E. L.; Safinya, C. R. *Appl. Phys. Lett.* **2000**, *77*, 313.

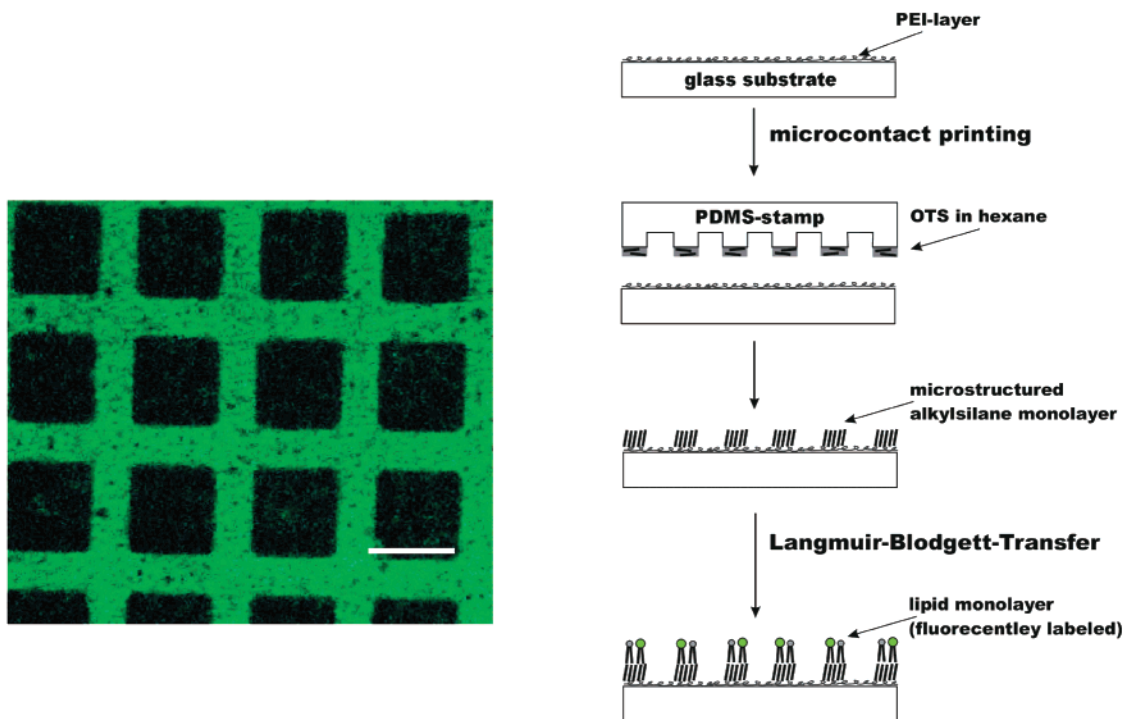


Figure 2. Confocal microscopy image of a microstructured surface prepared by printing a microstructured stamp on a flat PEI-coated glass substrate (bar, 10 μm). A fluorescently labeled lipid monolayer was transferred using the Langmuir–Blodgett technique onto the hydrophobic areas of the micropattern (green). The black specks in the transferred lipid monolayer are from solid lipid domains. The lipids labeled with the fluorescence dye are insoluble in the solid phase of the lipids.

Method II. First, the whole negatively charged silicon/silicon oxide surface was coated with PEI. For this, the substrate was immersed in a 1 mg/mL aqueous solution of PEI for 20 min and washed in three successive beakers of Millipore water (soaking time 1–2 min each). In the second step, an alkylsilane monolayer was printed on top of the PEI-coated microchannels, using microcontact printing of OTS (in hexane solution) with an additional stamp pad step (see method I). After removal of the stamp, the substrate was sonicated twice in ethanol for 2–3 min and then several times in Millipore water.

Microstructures on PEI-Coated Flat Substrates. Flat glass or silicon substrates were immersed in a 1 mg/mL aqueous solution of PEI for 20 min and washed in three successive beakers of Millipore water. A symmetric pattern of squares (PEI-coated squares, length of $\sim 10 \mu\text{m}$; alkylsilane frame, width of $5 \mu\text{m}$) was deposited on PEI-coated surfaces using a microstructured PDMS stamp inked with OTS (Figure 2). The microstructured PDMS stamp was cast from a photoresist pattern made in a standard photolithography process.^{28,29} By use of the Langmuir–Blodgett technique,^{30,31} a lipid monolayer of partially fluorescently labeled dimyristoyl-phosphatidylcholine (DMPC, Molecular Probes and Avanti Polar Lipids) was transferred onto the hydrophobic alkylsilane areas of this micropattern (film balance from Nima Technologies).

Contact Angle. All sessile drop contact angles of a $1 \mu\text{L}$ droplet of water were measured on flat silicon and glass surfaces with a CCD camera that was mounted on a telescope. For measurements on the alkylsilane monolayers deposited on silicon/silicon oxide as well as on PEI-coated substrates, flat PDMS stamps coated with OTS were printed on the planar surfaces.

Materials. Bovine brain microtubule protein was prepared, and tubulin was purified by phosphocellulose chromatography as described.³² Microtubule seeds were prepared by polymerizing $39 \mu\text{M}$ tubulin into microtubules in PEM buffer (100 μM Pipes,

1 mM MEGTA, 1 mM MgSO_4) containing 100 μM GTP, 10% glycerol, and 10% DMSO at 30°C for 30 min and sheared as described.³³ Tubulin (39 μM) was polymerized at the ends of the seeds after diluting the seeds 6-fold in PEM buffer containing 100 μM GTP. The final glycerol and DMSO concentrations were 1.67%. After 5 min of polymerization at 30°C , the microtubules were stabilized by the addition of taxol in increments of 2.5 μM at 5 min intervals to a final concentration of 7.5 μM taxol. The taxol-stabilized microtubules had an average length of approximately 10 μm . Calf thymus DNA (~ 2000 base pairs) was obtained from Life Technologies; high molecular weight calf thymus DNA ($\sim 75\,000$ base pairs), from Amersham Life Science; and the lipids DOTAP (dioleoyltrimethylammoniumpropane) and DOPC (dioleoylphosphatidylcholine), from Avanti Polar Lipids. The liquid crystals 5CB (4'-n-pentyl-4-cyanobiphenyl) and 8CB (4'-n-octyl-4-cyanobiphenyl) were purchased from Aldrich, and fluorescein was from Sigma.

Micromanipulator. The microinjection system, InjectMan and Transjector 5246 from Eppendorf, was used for the micro-manipulation experiments in individual microchannels. The manipulator system permits joystick-controlled movement and positioning of a micropipet in x -, y -, and z -directions with a step resolution of 157 nm. The filling and draining of liquids on the microstructured substrates were controlled by a compensation pressure in 8 hPa increments in the range of 0–2000 hPa. Micropipets in various shapes and with different tip diameters (0.5–20 μm) were prepared with a micropipet puller, P-97 from Sutter Instrument Co. The micromanipulator was mounted onto a Nikon Microphot FX upright microscope equipped for epifluorescence and polarization microscopy. A Peltier element was used for temperature control at the substrate. To vary the humidity, nitrogen was bubbled through a gas washing bottle containing water and was blown over the sample. Evaporation of solvent from dilute solutions was prevented by filling the microchannels through droplets of silicone, fluorosilicone (viscosity of 100–10000 cSt, Gelest), or polybutene oils (viscosity of 30–4000 cSt, Aldrich) placed on top of the substrate surface.

Laser Scanning Confocal Microscopy. The laser scanning confocal fluorescence microscopy measurements were performed

(28) Kumar, A.; Whitesides, G. M. *Appl. Phys. Lett.* **1993**, *63*, 2002.

(29) Kumar, A.; Biebuyck, H. A.; Whitesides, G. M. *Langmuir* **1994**, *10*, 1498.

(30) Blodgett, K. B.; Langmuir, I. *Phys. Rev.* **1937**, *51*, 937.

(31) Ulman, A. *An Introduction to Ultrathin Organic Films*; Academic Press: Boston, 1991.

(32) Panda, D.; Miller, H. P.; Wilson, L. *Proc. Natl. Acad. Sci. U.S.A.* **1999**, *96*, 12459.

(33) Farrell, K. W.; Jordan, M. A.; Miller, H. P.; Wilson, L. J. *Cell Biol.* **1987**, *104*, 1035.

with a Leica TCS MP confocal microscope equipped with a 0.5 W 1 ps pulse Ti:Sapphire laser for 2-photon excitation. The images were obtained in reflection and fluorescence modes, using the 488 nm line of an Ar laser and the 568 nm line of a Kr laser. A water immersion objective PL APO 63 \times 1.20 W was used. The z-axis was calibrated for depth measurements on the microchannels using profilometry. The high affinity DNA stain YOYO-1 iodide (excitation 491 nm/emission 509 nm; dye to base pair ratio 1:10) and Texas Red-DHPE (excitation 582 nm/emission 601 nm) used for fluorescence labeling (0.3 mol % fluorescence stain) of the DOPC/DOTAP liposomes were obtained from Molecular Probes and Avanti Polar Lipids, respectively.

Results

Surface Modification of the Microchannels. The wetting properties (hydrophobicity) of the treated surfaces were characterized by contact angle measurements. For an alkylsilane monolayer covalently bound to the silicon/silicon oxide surface (method I), the sessile drop contact angle of water was found to be $\theta_w^I = (80 \pm 10)^\circ$, whereas for dried PEI-coated surfaces the water contact angle was $\theta_w \sim 20^\circ$. For hydrophobic alkylsilane monolayers bound to the PEI-coated surfaces, a contact angle of $\theta_w^{II} = (90 \pm 5)^\circ$ was measured. These contact angles were smaller than the contact angle of a "perfect" monolayer prepared with OTS in a solution reaction ($\theta_w = 112\text{--}117^\circ$,^{34,35}) due to the fact that we used a dry stamp pad technique.¹⁷ The use of an additional stamp pad during the microcontact printing process was chosen to avoid capillary condensation and a chemical reaction between excess OTS and the channel walls. In comparison to the hydrophobic top monolayers, the hydrophilic walls and bottoms of the microchannels are only coated with cationic PEI layers (see Figure 6).

The stability of an alkylsilane monolayer printed on a polyelectrolyte that is electrostatically bound to the silicon/silicon oxide surface (method II) was tested with microcontact printing experiments on flat silicon and glass surfaces. A symmetric pattern of hydrophilic squares (PEI coated, length of $\sim 10 \mu\text{m}$) with hydrophobic frames (alkylsilane monolayer, width of $\sim 5 \mu\text{m}$) was prepared using a microstructured stamp for printing OTS on the PEI-coated substrates. For the visualization of this micropattern, a lipid monolayer of partially fluorescently labeled DMPC was transferred onto the hydrophobic frames using the Langmuir–Blodgett technique.^{30,31} The sample was then imaged with fluorescence and confocal microscopy (Figure 2). The roughness and the shape of the borderline between the hydrophilic PEI-coated areas and the fluorescently labeled lipid layer areas of the surface did not change for at least 1 week (sample was stored after preparation in air). The lateral stability of this microstructure is an indication that the electrostatic interaction between the negative charged surface and the PEI is not reduced due to the microcontact printing of an OTS monolayer on the polyelectrolyte. Furthermore, the lateral diffusion of the modified polyelectrolyte layer is below the optical resolution.

There are two possible mechanisms which could explain the interactions between the PEI and the OTS layers. Through the hydrolysis of OTS during the microcontact printing process, a strong hydrogen bonding between Si–OH groups and the amine groups of the PEI could be formed. This hydrogen bonding could be responsible for the observed strong interaction between the alkylsilane

monolayer and the polyelectrolyte. An alternative mechanism is the formation of a covalent Si–N bond. A covalent Si–N bond is easy to hydrolyze in water, but the sensitivity of hydrolysis is reduced by steric hindrance.³⁶ The decrease of the stability of alkylsilane layers on PEI-coated substrates for different storing conditions could be a hint that a covalent Si–N is formed.

The stability of the monolayer coated on flat substrates was tested with contact angle measurements. The contact angle θ_w of the alkylsilane monolayer on PEI did not change for a time period of 8 weeks ($\theta_w = \theta_w^I = (90 \pm 5)^\circ$) when the sample was stored in a dry environment. In contrast, a reduction of θ_w was found if the samples were stored in aqueous solutions for the same time duration: after storing in Millipore water (pH = 5.5), θ_w decreased by $\sim 10^\circ$, whereas in acidic (pH = 2) and basic (pH = 9.5) solutions θ_w decreased by $\sim 20^\circ$. This change of the monolayer hydrophobicity could be attributed to a slow hydrolysis of the Si–N bond in water and a faster hydrolysis in acidic or basic solution.

A comparison of the two surface modification methods demonstrated that the microstructures that are prepared with method I are more stable in aqueous solutions. No change of the contact angle θ_w^I could be observed after storing the modified substrates in water for a time period of 8 weeks. However, the advantage of using method II for surface modification is that a more hydrophobic top monolayer is formed under the same dry stamping conditions due to the intermediate polyelectrolyte layer between the silicon/silicon oxide surface and the alkylsilane layer. In addition, no polyelectrolyte can be adsorbed on the alkylsilane monolayer due to the different sequence of the preparation steps. Since the OTS can also be stamped on poly(allylamine hydrochloride) (PAH) with a similar stability as on PEI, lateral microstructured surfaces on layer-by-layer deposited multilayers with special physical and chemical properties can be produced.³⁷ Electrostatically deposited anionic polyelectrolytes, such as poly(sodium 4-styrenesulfonate) (PSS), can be used for changing the positive surface charge of the PEI-coated hydrophilic areas of the microstructures that are prepared using methods I or II.

Introduction and Manipulation of Material in Microchannels. The modified microchannels with contrasting wetting properties permit selective loading of macromolecular materials in the microchannels. Solutions, like aqueous solutions of biomaterials, can easily be introduced with macroscopic techniques (e.g., droplet evaporation, spin and dip coating) in such modified microchannels. Figure 3a shows the top view of a droplet of a dilute microtubule solution placed on a microchannel array modified using method I. Water from the microtubule solution is evaporating until the remaining solution is in equilibrium with the humidity of the surroundings. Such an equilibrium state of the microtubule solution is shown in Figure 3b. The hydrophilic microchannels are filled with concentrated microtubule solution (dark areas), and no solution remains on top of the microchannels. Furthermore, the microchannels contain most of the microtubules because hardly any adsorbed material on the hydrophobic top can be observed. During the evaporation process, the solution is observed to flow along the channels (see figure). With this technique, it is possible to directly deposit biomaterial solutions into microchan-

(34) Cohen, S. R.; Naaman, R.; Sagiv, J. *J. Phys. Chem.* **1986**, *90*, 3054.

(35) Bierbaum, K.; Grunze, M.; Baski, A. A.; Chi, L. F.; Schrepp, W.; Fuchs, H. *Langmuir* **1995**, *11*, 2143.

(36) Pawlenko, S. *Organo-Silicon-Compounds*. In *Houben-Weyl, Methods of Organic Chemistry*, Vol. XIII/5; Georg Thieme Verlag: Stuttgart, 1980; pp 226–230.

(37) de Gennes, P. G.; Prost, J. *The Physics of Liquid Crystals*; Oxford University Press: New York, 1995.

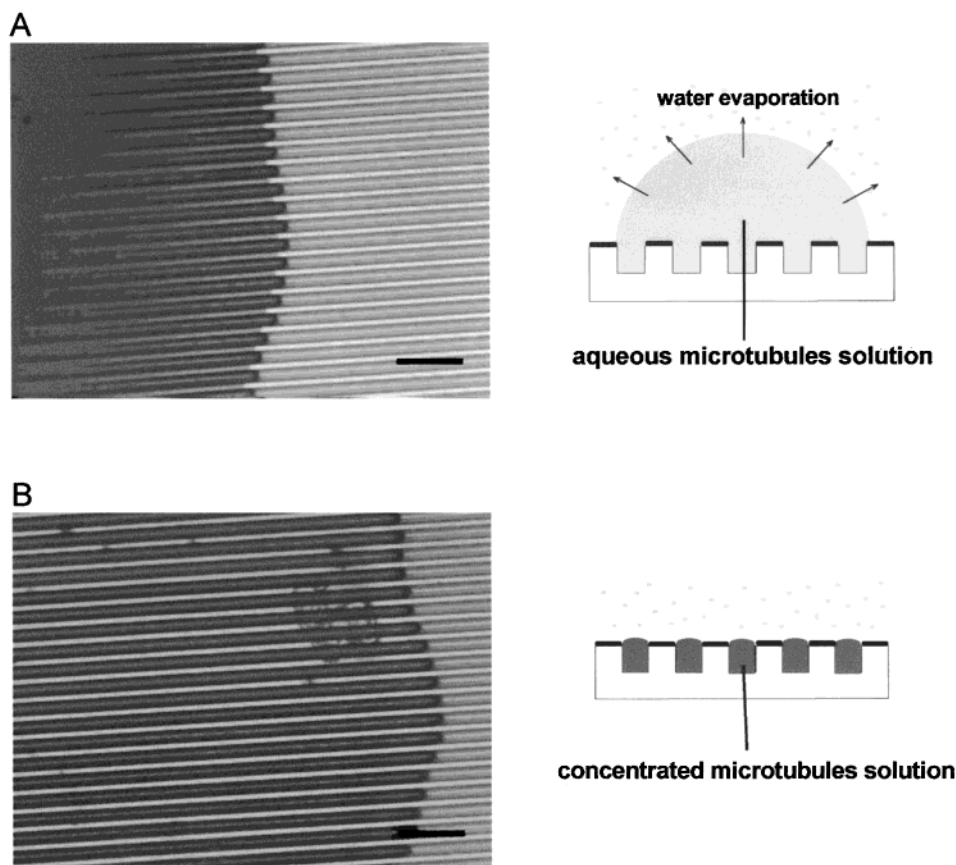


Figure 3. (A) Optical micrograph of a droplet of microtubule solution (0.5 mg/mL) on top of a surface-modified (method I) microchannel array (top view; bar, 20 μm). The contact line of the microtubule solution in the microchannels runs in front of the macroscopic droplet (darker areas). (B) Optical micrograph of the droplet on top of the lithographic surface ~ 30 min later. The main droplet has evaporated, and a more concentrated microtubule solution in equilibrium with the humidity of the surrounding atmosphere is located only in the microchannels. During the evaporation process, a slow flow of the droplet front can be observed.

nels and to prepare highly concentrated samples (> 20 mg/mL) for optical investigations and X-ray measurements. In comparison, concentrated biomaterial solutions cannot be stabilized on microchannels with an unmodified silicon/silicon dioxide surface. Because of the small contact angle of the solution on this surface ($< 5^\circ$), a placed droplet wets the entire surface. The process of water evaporation on a silicon/silicon oxide surface is much faster than on a modified surface, and after evaporation randomly adsorbed biomaterials are observed on top and in the microchannels.

A microinjector system was applied for the controlled filling and manipulation of materials in a single surface-modified microchannel. For this, a microtip was placed into a single channel and the injection system allows precise control of the volume of transferred solution. Repeating this transfer step with different solutions results in the ability to mix several compounds in a single microchannel. Channels with a smaller width than the diameter of a microtip ($< 0.5 \mu\text{m}$) can be filled by placing a small droplet with the micromanipulator on the hydrophobic top that is in contact with a microchannel. The solution flows into the channels due to the capillary force. Afterward, the droplet on top of the single microstructure can be removed.

We developed three different methods for sample deposition, as sketched in Figure 4, to accommodate the requirements of different applications. Investigations of nonvolatile liquids need no further improvements from the procedure described above (Figure 4a). The volume of liquid microstructures can be controlled with a micromanipulator on surface-modified microchannels. By use

of liquid crystals and silicone oils, experiments on the influence of confinement and on the wetting behavior of liquid microstructures^{10,13} can be carried out.

The introduction and alignment of biomaterials in microchannels is much more difficult since these materials need to remain in a solution. To avoid water evaporation, drying, and denaturation of the biomaterials, these aqueous solutions have to be stabilized by controlling the humidity or adding salt. Another problem is the high viscosity of concentrated biomaterial solutions (e.g., high molecular weight DNA), which impedes flow in the microtip and channels. To successfully fill a microchannel with these solutions using a microtip, the solutions have to be diluted. However, the concentration of the biomaterial solution in filled channels can be increased by changing the humidity of the environment and thus causing excess water to evaporate (Figure 4b). Using this method, it is possible to prepare biomaterial samples that have a much higher concentration than the initial solution. An example of concentrated DNA solutions in microchannels is shown in the micrographs of Figure 4b. By use of the microinjection technique, two microchannels were filled with a solution of short-stranded DNA (~ 2000 base pairs, filled dark channels on image 1 of Figure 4b) and three channels were filled with a solution of long-stranded DNA ($\sim 75\,000$ base pairs, filled white channels on images 1 and 2). Since each of these channels can be filled independently and the composition of compounds can be controlled in a single microchannel, 400 samples of highly concentrated biomolecular materials on a $1 \text{ mm} \times 1 \text{ mm}$ device of microchannels with a width of $1.5 \mu\text{m}$ can be produced for optical microscopy and X-ray experiments.

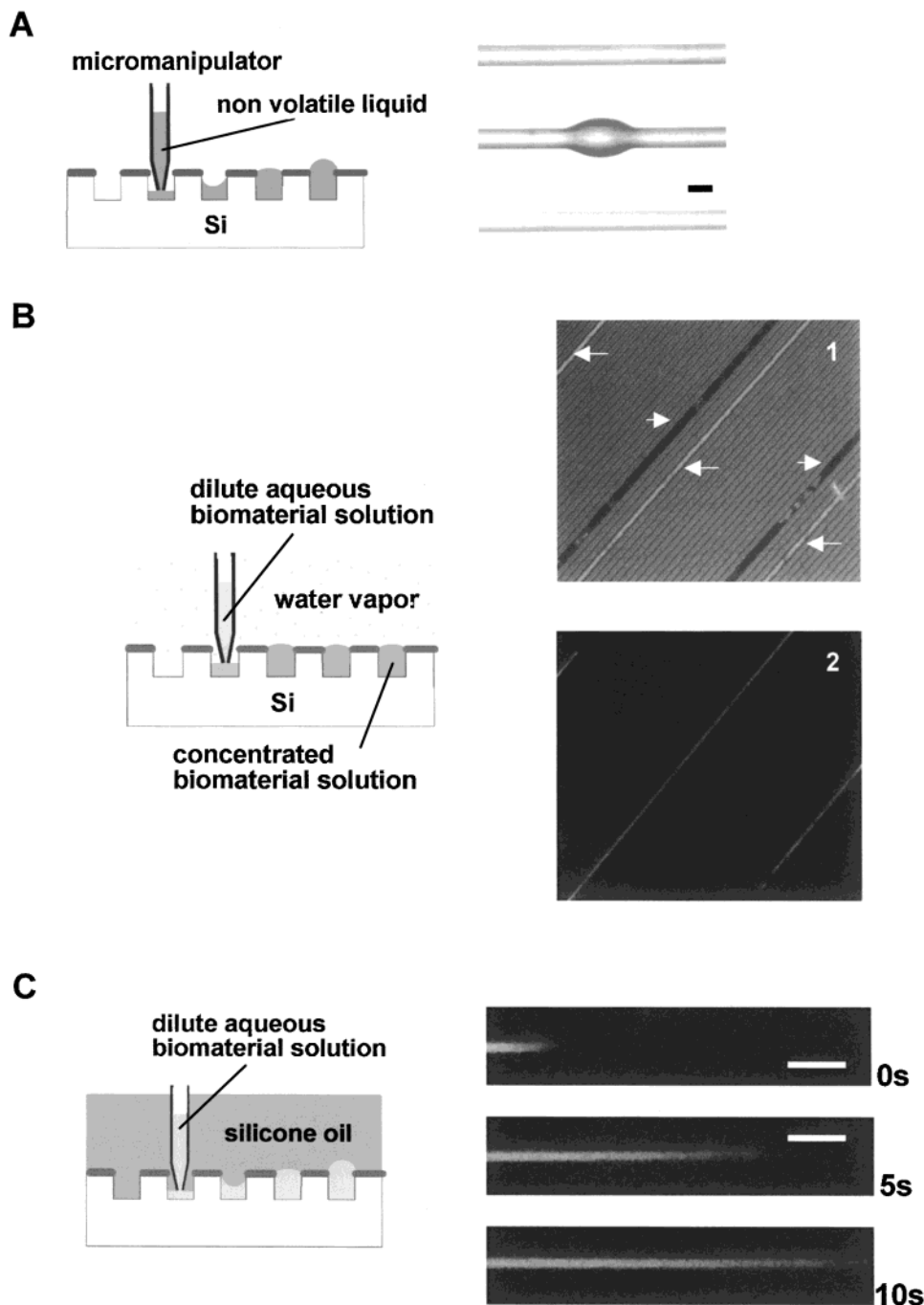


Figure 4. Sketches and micrographs of the application of a micromanipulator under different experimental conditions. (A) Filling microchannels with nonvolatile liquids: The micrograph shows microchannels which were filled with different amounts of 5CB (bar, $20\ \mu\text{m}$). The middle channel has become unstable (ref 10), forming a droplet on the microchannel. (B) Filling microchannels with biomolecular material solutions: Highly concentrated DNA solutions with different strand lengths, ~ 2000 base pairs (two black channels on image 1) and $\sim 75\ 000$ base pairs (three white channels on images 1 and 2), were loaded in the microchannels with a micromanipulator and observed under crossed-polarizers. The first image shows the polarization microscopy image of the biomaterials under air (bar, $20\ \mu\text{m}$). A weak signal of the empty microchannels can be also observed. When the air atmosphere is replaced with silicone oil, only light from the aligned material (DNA strand length of $\sim 75\ 000$ base pairs) can be detected (image 2). When the sample is rotated by 45° , no signal is observed for the long-stranded DNA due to the fact that the DNA is oriented along the channels. (C) Filling microchannels with dilute aqueous solution under silicone oil: Diffusion of fluorescein in a microchannel filled with water under an oil atmosphere at different times (channel width, $5\ \mu\text{m}$).

Due to the different composition of material in each microchannel, such microchannel devices can be used for combinatorial investigations in chemical and biological science.

Filling the microchannels under an atmosphere of inert oil (silicone oil, polybutene oil) is a third way of stabilizing liquid microstructures (Figure 4c). The advantage of this method is the ability to precisely control the concentration of the solution. Since the solvent is insoluble in the oil, the

solution of the filled microchannel has exactly the same concentration as the initial solution. This exact control of the concentration, especially for very dilute solutions, cannot be obtained under humid air conditions. Furthermore, volatile organic solvents and water/organic solvent mixtures can be filled in the microstructures as long as they are insoluble in the surrounding oil. This method can be also used for dynamic experiments of small and large molecules under geometric and surface energy

constraints as is shown for the example of fluorescein diffusion in water in the micrographs in Figure 4c.

Confinement and Alignment of Macromolecules in Microchannels. The combination of geometric confinement and capillary flow during sample loading induces linear alignment of long-chain biological macromolecules such as DNA and the cytoskeletal microtubules. A particular case is microtubules, which can be considered essentially as rigid rods (diameter of >20 nm, persistence length of >10 μm). Because the lengths of the microtubules approach or exceed the width of the channels, they are expected to align along the channels. For less rigid biomaterials such as DNA (persistence length of ~ 100 nm), linear alignment of the DNA molecules (in a highly concentrated DNA solution) can be observed as the contour length of the chain approaches the channel widths. For example, short-stranded DNA (~ 2000 base pairs, contour length of ~ 700 nm) did not show any alignment of the DNA phase in microchannels with a width of 1.5 μm (two black channels on image 1 of Figure 4b). In comparison, longer stranded DNA ($\sim 75\,000$ base pairs, contour length of ~ 26 μm) shows alignment of the highly concentrated DNA solution (white channels on images 1 and 2 of Figure 4b). The near complete extinction of the light when the sample was rotated by 45° with respect to the image 2 suggests linear alignment of the long-stranded DNA along the channel direction. Since the DNA molecules are in a highly concentrated phase (the hexagonal phase of DNA as revealed by the defect structure of unoriented samples in large width channels), we expect that this mesoscale phase should spontaneously orient along the channels as we observe once the contour length of DNA (the building blocks of the phase) approaches the channel width.

The alignment of biomaterials and filamentous proteins inside the microchannels, which at certain conditions may acquire crystalline order, presents a good opportunity for studying the structures of these materials, which are intrinsically difficult to crystallize in three dimensions, by high-intensity X-ray diffraction. Since these molecules are kept in a hydrated state, the biological activity of the biomaterials in the microchannels is maintained. However, the finite thickness and width of the samples (hence small volume) present some challenges in obtaining sufficient X-ray scattering signal using conventional X-ray diffraction methods. We are currently developing X-ray microdiffraction methods utilizing a linearly focused X-ray beam with a focus size smaller than the channel width^{19,20} to characterize these samples.

Confinement of Liquid Crystals in Microchannels. The control of mesoscale defect structures of liquid crystals is important for many technological applications (e.g., liquid crystal displays). The spatial modulation introduced by microchannels is expected to directly influence the defect structures because of similar length scales. We studied confinement of the rodlike thermotropic liquid crystal 8CB (4'-n-octyl-4-cyanobiphenyl, molecule length of ~ 3 nm) in microchannels. For these experiments, PEI-coated microchannels of different widths (20 and 3 μm) and a depth of ~ 2 μm were filled with 8CB using a micromanipulator. The defects were observed under a microscope using crossed polarizers. The images are shown in Figure 5. For comparison, a bulk droplet of the liquid crystal placed on flat PEI-coated silicon substrate is also shown. 8CB has a transition at 21.5 $^\circ\text{C}$ from a crystalline to a smectic A phase, at 33.5 $^\circ\text{C}$ to a nematic phase, and at 40.5 $^\circ\text{C}$ to an isotropic phase.³³ The nematic phase has long-range orientational order with the rod-shaped molecules all pointed on average in the same direction. The molecules, however, exhibit liquidlike positional order.

In the smectic A phase, the rod-shaped molecules segregate into stacks of liquidlike layers. The smectic A phase thus has one-dimensional positional order along the direction perpendicular to the layers.

The polarized microscopy images on the left (Figure 5) show the liquid crystal in the nematic phase. The threadlike texture of the nematic phase can be clearly seen.³⁴ The confining width of the microchannels leads to a defect structure on a much smaller length scale than in bulk liquid crystal films.³⁵ Upon cooling the samples below the smectic A–nematic phase transition temperature, an unexpected defect structure of the smectic A phase was observed as shown in the micrographs on the right-hand side of Figure 5. This structure consisted of a collection of distorted spherulite-like domains in which the layers of the liquid crystal molecules are aligned in onionlike distorted concentric spheres. Spherulites are a particular type of defect structures with positive Gaussian curvature. Although they are readily observed in multilayer membrane systems, they are rarely observed in smectic A liquid crystals.³⁶ Some classical focal conic defects (where the layers form a toruslike structure) with negative Gaussian curvature are also evident.^{37,38} The size distributions of the spherulite and toruslike domains in these 20 μm microchannels, while not perfectly monodisperse, already show the effects of confinement and are surprisingly not too polydisperse. In comparison to the confined liquid crystal in microchannels of 20 μm width, the bulk droplet of 8CB shows larger domains in the smectic A phase. When the channel width is reduced from 20 to 3 μm , a surprisingly different texture is observed in the smectic A phase. The 8CB layers are mainly aligned parallel to the bottom walls of the channels and are accompanied by an orientation of the long molecular axes normal to the bottom surface. The aligned areas (dark under crossed polarizers) are partly interrupted by defect spherulite-like or toruslike regions which allow light through the crossed polarizers. In comparison to the defect structures observed in the 20 μm channels, these defect domains are seen to have a uniform size, which is controlled by the channel width. Thus, through confinement on a mesoscale, the defect structure and the domain size of liquid crystals can be manipulated and controlled. These different defect structures are known to result in a change in material properties, for example, the rheological (elastic and viscous) properties. For example, while oriented smectic A phases of liquid crystals have little resistance to flow as long as the layer normal is not along the velocity direction, spherulite-like smectic A materials exhibit a large elastic modulus in response to resistance due to layer distortions, that is, they behave like soft solids.^{39,40} Geometric constraints for the control of the mesoscopic structure and material properties may be used for other materials such as block copolymers and lyotropic liquid crystals. We note that a number of earlier studies^{41–44} have looked at the effect of grooves and gratings on liquid crystal alignment. Here, we present patterned surfaces where we control the surface chemistry

(38) Chandrasekhar, S. *Liquid Crystals*, Cambridge University Press: New York, 1992.

(39) Safinya, C. R.; Sirota, E. B.; Plano, R. J. *Phys. Rev. Lett.* **1991**, *66*, 1986.

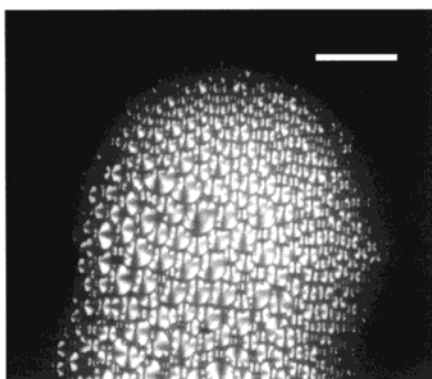
(40) Safinya, C. R.; Sirota, E. B.; Bruinsma, R. F.; Jeppesen, C.; Plano, R. J.; Wenzel, L. J. *Science* **1993**, *261*, 588.

(41) Kawata, Y.; Takatoh, K.; Hasegawa, M.; Sakamoto, M. *Liq. Cryst.* **1994**, *16* (6), 1027.

(42) Newsome, C. J.; O'Neill, M.; Farley, R. J.; Bryan-Brown, G. P. *Appl. Phys. Lett.* **1998**, *72*, 2078.

(43) Hallam, B. T.; Sambles, J. R. *Liq. Cryst.* **2000**, *27* (9), 1207.

(44) Smela, E.; Martinez-Miranda, L. J. *J. Appl. Phys.* **1993**, *3299*.

Droplet:

smectic phase

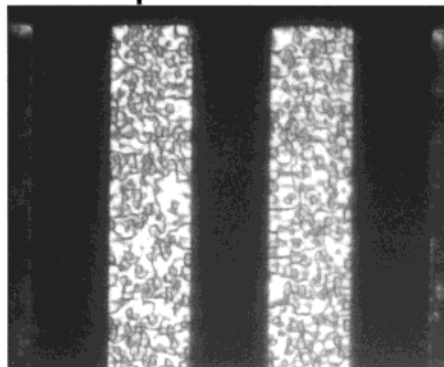
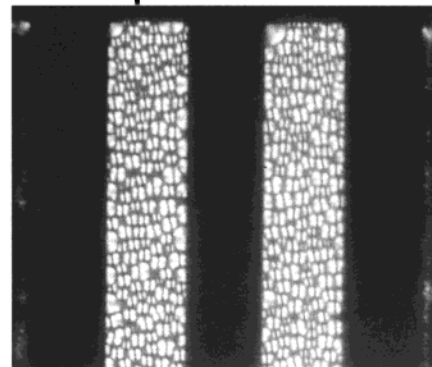
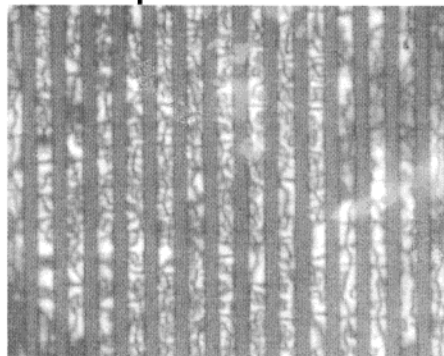
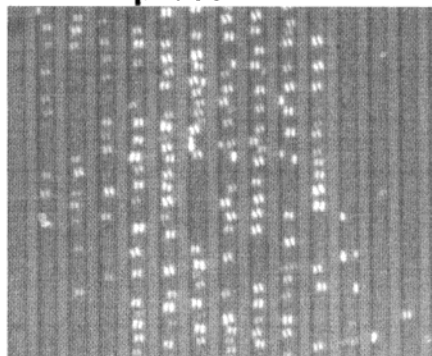
20 μ m:**nematic phase****smectic phase****3 μ m:****nematic phase****smectic phase**

Figure 5. A small liquid crystal droplet (8CB) on a PEI-coated silicon substrate (bar, 20 μ m) and confined in microchannels with different widths (20 and 3 μ m). The left micrographs show the topology of 8CB in the nematic phase; the right ones show the topology in the smectic A phase (polarization microscopy).

by a combination of hydrophobic tails and charged polymers.

Confocal Microscopy Characterizations. Laser scanning confocal microscopy was used to image the three-dimensional shape of liquid microstructures in the microchannels. A confocal microscope image of the wetting behavior of highly concentrated biomaterials in microchannels is shown in Figure 6. This image is an overlay of the reflection mode image with two fluorescence mode images with different colors. The scanning direction is the x - z plane parallel to surface normal. The surface structures of the microchannels can be clearly imaged through reflected signal from the top and the bottom of the channels. The steepness of the channel walls that are

showing no reflected confocal signal can be estimated from the dark areas between the reflections from the top and the bottom of the channels. The microchannel substrate was modified using method II. A liposome solution of the cationic lipid DOTAP (40 wt %) and the neutral lipid DOPC (60 wt %) labeled with a fluorescence dye (red in Figure 6) and a solution of high molecular weight calf thymus DNA stained with a different fluorescence stain (blue in Figure 6) were used to partly fill the microchannels using a micromanipulator. The samples were prepared under normal laboratory humidity conditions. Since evaporation was occurring during the filling process, the final concentration of the biomaterial solutions in the microchan-

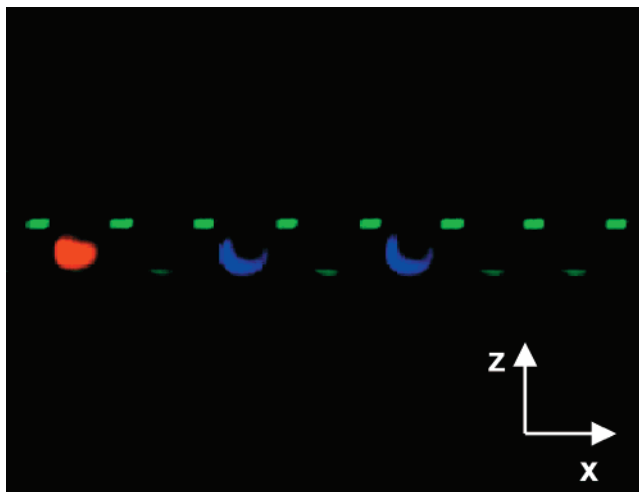


Figure 6. Confocal microscopy scan in the x - z direction of microchannels which are partly filled with cationic liposomes (red) and DNA (blue). This image is an overlay of the reflection mode (green) with two different fluorescence modes (bar, 10 μm).

nels is much higher than in the original solutions. Therefore, the imaged shapes (in the x - z plane) of the biomaterial solutions present more the adsorption or coating behavior due to the interactions between these complex liquids and the PEI-coated walls during the partial evaporation of water than the wetting behavior of a simple liquid. After filling the microchannels, the entire substrate was covered with silicone oil to avoid further water evaporation during the imaging experiments. The interactions between the two biomaterial solutions containing cationic liposomes and DNA and the PEI-coated walls of the microchannels are unambiguously different. The cationic liposome solution does not wet the cationic PEI-coated walls, whereas the DNA solution coats the positive charged walls due to the attractive electrostatic interactions of cationic PEI and anionic DNA. The uneven spreading of the materials in the microchannels (more material on the left side) is an effect of the micromanipulator being tilted during sample filling. The wetting behavior of different biomaterials in microchannels as imaged by confocal microscopy clearly showed that the surface charge of the microchannel walls is positive due to the adsorption of PEI.

Conclusions and Outlook

We have developed a series of methods for creating and manipulating microstructures with distinct chemical and physical properties for the purpose of confining biopolymers and liquid crystals. The surface wettability, charge, reactivity, and biocompatibility can be controlled with microcontact printing and polyelectrolyte adsorption. In

particular, microcontact printing on PEI-coated lithographic silicon substrates is a simple new process to get the desired surface properties. The micromanipulation technique allows us to control the volume and composition in a single microchannel that provides a promising tool for combinatorial structural analysis in chemistry and biology. Concentrated solutions of biomaterials such as DNA and microtubules have been confined and oriented in these microstructures. The ability to orient these biomolecular materials leads to highly ordered systems for microscopy and above all for X-ray investigations which will allow high-quality structure characterization of biological macromolecules which generally show poor interpretative features in unoriented samples. It is expected that by using a microfocused X-ray beam at a third generation synchrotron source, measurements on single bundles of cytoskeletal proteins and DNA may be performed. The influence of geometric constraints on the mesoscopic defect structure of liquid crystals has been also shown for 8CB. By variation of the width of the channel, the defect structure and the size distribution of the defects can be controlled. By use of laser scanning confocal microscopy, the wetting behavior of complex biomaterials and their interactions with positive charged walls of the microchannels were studied. The development of the surface modification techniques as well as methods for manipulating and characterizing biomaterials inside microchannels provides the basis for technological applications incorporating complex materials in microfabricated device structures, such as in biological and chemical sensors.

Acknowledgment. We gratefully acknowledge useful discussions with Karlheinz Graf, Tilo Pompe, Ralf Seemann, Markus Seitz, and Nelle Slack. We are indebted to Myung Chul ("MC") Choi for providing the image of the 8CB droplet. We especially acknowledge many discussions on confined fluid films with Jacob Israelachvili. We thank Gernot Wirnsberger for help with the preparation of structured PDMS stamps and Elaine Haberer for assistance with the profilometry measurements. This work was supported by National Science Foundation Grants DMR-9972246 and DMR-0076357, National Institutes of Health Grants GM59288 and NS13560, Office of Naval Research Grant N00014-00-1-0214, and the University of California Biotech Research and Education Program Training Grant 99-14. The Materials Research Laboratory at UC-Santa Barbara is supported by NSF-DMR-0080034. T.P. acknowledges support by a DFG (Pf 375/1-1) scholarship. Y.L. acknowledges a visiting scholar fellowship from Chongqing University, China. M.W.K. acknowledges partial support by KISTEP (99-I-01-03-A-064).

LA010145Z